Cell Cycle 13:5, 859–868; March 1, 2014; © 2014 Landes Bioscience

De novo fatty acid synthesis at the mitotic exit is required to complete cellular division

Natalia Scaglia[1,†], Svitlana Tyekucheva[2,3], Giorgia Zadra[1,4], Cornelia Photopoulos[1], and Massimo Loda[1,4,5,6,7,*]

[1]Department of Medical Oncology; Dana-Farber Cancer Institute; Harvard Medical School; Boston, MA USA; [2]Department of Biostatistics and Computational Biology; Dana-Farber Cancer Institute; Boston, MA USA; [3]Department of Biostatistics; Harvard School of Public Health; Boston, MA USA; [4]Department of Pathology; Brigham and Women's Hospital; Harvard Medical School; Boston, MA USA; [5]Center for Molecular Oncologic Pathology; Dana-Farber Cancer Institute; Harvard Medical School; Boston, MA USA; [6]The Broad Institute; Cambridge, MA USA; [7]Division of Cancer Studies; King's College London; London, UK

[†]Current affiliation: Instituto de Investigaciones Bioquímicas de la Plata; Consejo Nacional de Investigaciones Científicas y Técnicas; Facultad de Ciencias Médicas; Universidad Nacional de La Plata; La Plata, Buenos Aires, Argentina

Keywords: fatty acid, phospholipid, lysophospholipid, cell cycle, de novo lipogenesis, AMPK, metabolome, cell cycle arrest, C75

Abbreviations: ACC, acetyl-CoA carboxylase; AMPK, 5′ AMP-activated kinase; 2TB, double thymidine block; FA, fatty acids; LysoPC, lysophosphatidylcholine; LysoPE, lysophosphatidylethanolamine; LysoPL, lysophospholipids; PL, phospholipids

Although the regulation of the cell cycle has been extensively studied, much less is known about its coordination with the cellular metabolism. Using mass spectrometry we found that lysophospholipid levels decreased drastically from G_2/M to G_1 phase, while de novo phosphatidylcholine synthesis, the main phospholipid in mammalian cells, increased, suggesting that enhanced membrane production was concomitant to a decrease in its turnover. In addition, fatty acid synthesis and incorporation into membranes was increased upon cell division. The rate-limiting reaction for de novo fatty acid synthesis is catalyzed by acetyl-CoA carboxylase. As expected, its inhibiting phosphorylation decreased prior to cytokinesis initiation. Importantly, the inhibition of fatty acid synthesis arrested the cells at G_2/M despite the presence of abundant fatty acids in the media. Our results suggest that de novo lipogenesis is essential for cell cycle completion. This "lipogenic checkpoint" at G_2/M may be therapeutically exploited for hyperproliferative diseases such as cancer.

While regulation of cell cycle progression has been extensively studied, most of the metabolic needs at different phases of the cell cycle and how the cells fulfil the metabolic requirements of cell division remain elusive.

Phospholipids (PL) are essential constituents of all membranes, and their content must therefore be duplicated during the cell cycle. The synthesis and turnover of the main PL in mammalian cells, phosphatidylcholine, occurs throughout the cell cycle with maximal net accumulation during the S phase, to support cellular growth.[1-3] Numerous studies have contributed to the understanding of the mechanisms that regulate phosphatidylcholine metabolism during G_1 and S[4-8] and its importance to surpass the G_1/S boundary.[9,10] The importance of PL synthesis and turnover in other phases of the cell cycle is less well known.

At the end of mitosis, many processes involving membrane expansion and remodeling take place. The addition of surface during cellular division has long been recognized, and it has been studied in a variety of organisms, including mammals.[11-13] Despite the importance of vesicular trafficking as a mean of surface membrane delivery, the source of this membrane is less well known. It has been shown that previously internalized plasma membrane is recycled to the cell surface as the cells divide;[13] however, de novo synthesis and degradation of different PL at the end of mitosis has also been documented.[7,14-16] In addition, nuclear envelope reassembly and expansion occurs upon mitotic exit and involves extensive membrane reorganization.[17,18]

Fatty acids (FA) are essential building blocks of PL, thus a correct supply is required for membrane synthesis. Cancer cells engage in an increased de novo FA synthesis as part of their anabolic reprogramming to support proliferation.[19-21] However, whether the endogenous synthesis of FA is regulated in a cell cycle-dependent manner is currently not known. Fatty acids, mainly palmitic acid, are synthesized endogenously by the consecutive action of 2 enzymes: acetyl-CoA carboxylase 1 (ACC) and fatty acid synthase (FASN). The rate-limiting enzyme of this pathway, ACC, is negatively regulated by palmitic acid. Interestingly, accumulation of free palmitic acid impairs cytokinesis in cancer and normal cells.[22] ACC is also inhibited by 5′ AMP-activated kinase (AMPK). In addition to its well-established role as a metabolic regulator, AMPK has been recently implicated in mitosis progression.[23] Furthermore, the activity of SREBP1, a major transcriptional regulator of lipogenic genes, is enhanced by hyperphosphorylation in mitosis.[24,25] Together,

*Correspondence to: Massimo Loda; Email: massimo_loda@dfci.harvard.edu
Submitted: 09/11/2013; Revised: 01/06/2014; Accepted: 01/08/2014; Published Online: 01/13/2014
http://dx.doi.org/10.4161/cc.27767

these observations suggest that lipogenesis may be differentially regulated at the mitotic exit.

The importance of cellular metabolism for proliferation has gained new interest because of its role in supporting transformation and its potential in being targeted for treatment.[26] Recent evidence suggests that the core machinery that regulates cell cycle progression is involved in cellular metabolic programming, in addition to the well-established regulation of nucleotide synthesis.[8,25,27-30] A better knowledge of the metabolic requirements during the cell cycle may help to identify new targets for cancer treatment and to design the schedule of combined therapies.[31] Here, we show that cells engage in an active membrane synthesis at the mitotic exit that is necessary to complete the cell cycle.

Results

Metabolic profiling reveals cyclic changes in several metabolic pathways

To screen for metabolic changes during the cell cycle, a metabolic profiling by LC-MS/GC-MS in double thymidine block (2TB)-synchronized HeLa cells was performed. Sixty-nine metabolites were found to be different across the various phases of the cell cycle (**Table S1**; **Fig. S1**). **Figure 1A** shows the distribution of the biochemical classes/pathways they belonged to. Among the most represented pathways that differed across the cell cycle were those related to polyamine, LysoPL, and glucose metabolism (**Fig. 1A**; **Fig. S1**). Several enzymes of polyamine and glucose metabolism have been previously shown to be regulated in a cell cycle-dependent manner.[28,32,33] Encouragingly, most of the metabolites belonging to these pathways were also found to be cyclic in our profiling, suggesting that our model was suitable for identifying cell cycle-regulated pathways.

More than 20% of the metabolites that differed across the cell cycle were LysoPL (**Fig. 1B**; **Fig. S1**). Both lysophosphatidylcholines (LysoPC) and lysophosphatidylethanolamines (LysoPE) were abundant. Of particular interest, the LysoPC and LysoPE showed higher values at G_2/M than at G_1 phase of the cell cycle, irrespective of their levels at S phase. Glycerophosphorylcholine and glycerophosphoethanolamine, degradation products of LysoPC and LysoPE, respectively, were unchanged during the cell cycle, suggesting that the reacylation of LysoPL to form new PL (**Fig. 1C**) increased from G_2/M to G_1. Moreover, glycerol-3 phosphate level (a substrate for de novo PL synthesis) also decreased from G_2/M to G_1 (**Fig. S1**), further suggesting that important changes in membrane metabolism occur in this period of the cell cycle.

The decrease in LysoPL content is accompanied by an augmented membrane synthesis as the cells reach G_1

The bulk of phosphatidylcholine is synthesized de novo by the CDP–choline pathway. We estimated the rate of phosphatidylcholine synthesis during the cell cycle. As expected, the incorporation of [^{14}C] choline into the lipids peaked as the cells progressed from G_2/M (8 h) to G_1 (10 h) phase of the cell cycle (**Fig. 2A**). The synthesis of phosphatidylcholine decreased slightly when the cells were pulsed during G_1 (10 to 12 h), and the lowest levels were seen at S and G_2/M phases (4 and 8 h, respectively). Interestingly, the maximal incorporation of choline did not correspond to the peak of any phase of the cell cycle (**Fig. S2A–D**), but rather the time when the cell number doubled, suggesting that the cells synthesized membranes during cellular division. Importantly, these changes were independent of cellular size or protein content (**Fig. S3A**). Moreover, the total FA content per cell at G_1, which represents mainly those acylated in PL, was more than half of the total FA content of those at G_2/M,

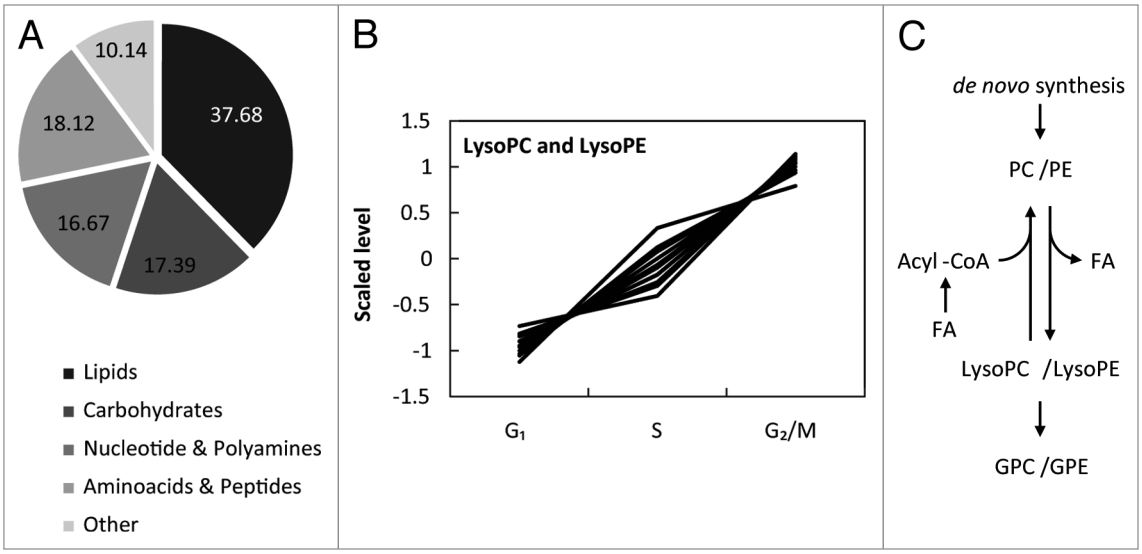

Figure 1. Metabolic profiling reveals extensive changes in metabolite levels during the cell cycle. HeLa cells were synchronized by 2TB and the metabolite levels, at different time points after the release, were obtained by GC/MS or LC/MS and normalized to total protein content. The levels of the metabolites at different phases of the cell cycle were deconvoluted using FACS data as described under "Materials and Methods". (**A**) Distribution of the cyclic metabolites in biochemical classes and (**B**) relative levels of the lysophosphatidylcholine (LysoPC) and lysophosphatidylethanolamine (LysoPE) species. (**C**) Schematic model of PC/PE metabolism. FA, fatty acids; PC, phosphatidylcholine; PE, phosphatidylethanolamine; GPC, glycerophosphorylcholine; GPE, glycerophosphoethanolamine.

indicating that the net accumulation of lipids occurred upon cell division, either late in mitosis or early in G_1.

De novo fatty acid synthesis increases as the cells divide

Both LysoPL reacylation and de novo PL synthesis require FA. Thus, we estimated the de novo FA synthesis during the cell cycle in synchronized cells. Acetate incorporation into lipids peaked when the cells were pulsed from G_2/M to G_1 (8 to 10 h) (**Fig. 3A**), and the overall pattern resembled the one for choline incorporation (**Fig. 2**). Accordingly, approximately 80% of the total acetate incorporated was used for PL synthesis (**Fig. 3B**). In addition, acetate relative distribution was also slightly changed at 10 h, with a higher channeling of FA toward PL at the expense of neutral lipids (**Fig. 3B**).

One of the main physiological sources of acetyl-CoA for FA synthesis is glutamine. As observed with acetate, the incorporation of [^{14}C] glutamine into lipids peaked as the cells divided (**Fig. S3B**), and, as before, most of the radiolabel was associated with FA (**Fig. 3C**). The incorporation of [^{14}C] glutamine into lipids was also increased upon cell division in thymidine–nocodazole-synchronized cells (**Fig. S3C**).

In addition to their de novo synthesis, cells incorporate FA from the extracellular milieu. However, unlike de novo FA synthesis, the uptake of exogenous radiolabeled palmitic acid did not change during the cell cycle in HeLa cells (**Fig. 3D**).

Overall, these results show that de novo FA synthesis increased during the cellular division to support membrane production, while the utilization of exogenous FA is unchanged.

Endogenously synthesized fatty acids are required to complete cellular division

To determine the importance of the increase in FA synthesis for cell cycle progression, we incubated HeLa cells with C75, an inhibitor of fatty acid synthase, under conditions that decreased FASN activity approximately 70% (**Fig. 4A**). C75 caused a marginal decrease in viability (≤20% in different experiments, data not shown) and a marked enrichment in the G_2/M population, as assessed by flow cytometry in HeLa cells (**Fig. 4B**). C75 caused a similar increase of cells with 4N amount of DNA in other cell lines (**Fig. S4A**). Cyclin B1 level was markedly increased in C75-treated HeLa cells (**Fig. 4C**), whereas cyclin A, which is degraded earlier than cyclin B1,[34] showed no changes, suggesting that the inhibition of FA synthesis arrested the cells at mitosis before ana/telophase.[35] Moreover, ~10% of the viable cells were recovered in the conditioned media (data not shown), and they showed high levels of cyclin B1, in keeping with the known looser attachment to the substrate during mitotic rounding (**Fig. 4C**, conditioned media).

It is worth noting that C75 treatment was done in the presence of 10% FBS, thus plenty of FA were available to the cells from the media. Consistently, the depletion of lipids from the media had no effect on the cell cycle distribution in asynchronous (**Fig. 4D**, inset) or synchronized populations (**Fig. S4B**). Even a long-term deprivation of exogenous lipids had no significant impact on proliferation (**Fig. 4D**). Moreover, the addition of exogenous palmitic acid was unable to rescue the cell cycle arrest (**Fig. S4C**). Thus, HeLa cells required endogenous fatty acid synthesis to complete cellular division.

AMPK activity toward ACC decreases at the mitotic exit

To evaluate possible regulatory mechanisms for the observed metabolic changes, we measured the mRNAs of different lipogenic enzymes, as well as that of some important ones for cytosolic NADPH production and Krebs cycle, during the cell cycle. We found no changes in the mRNA level (**Fig. S5**) or the

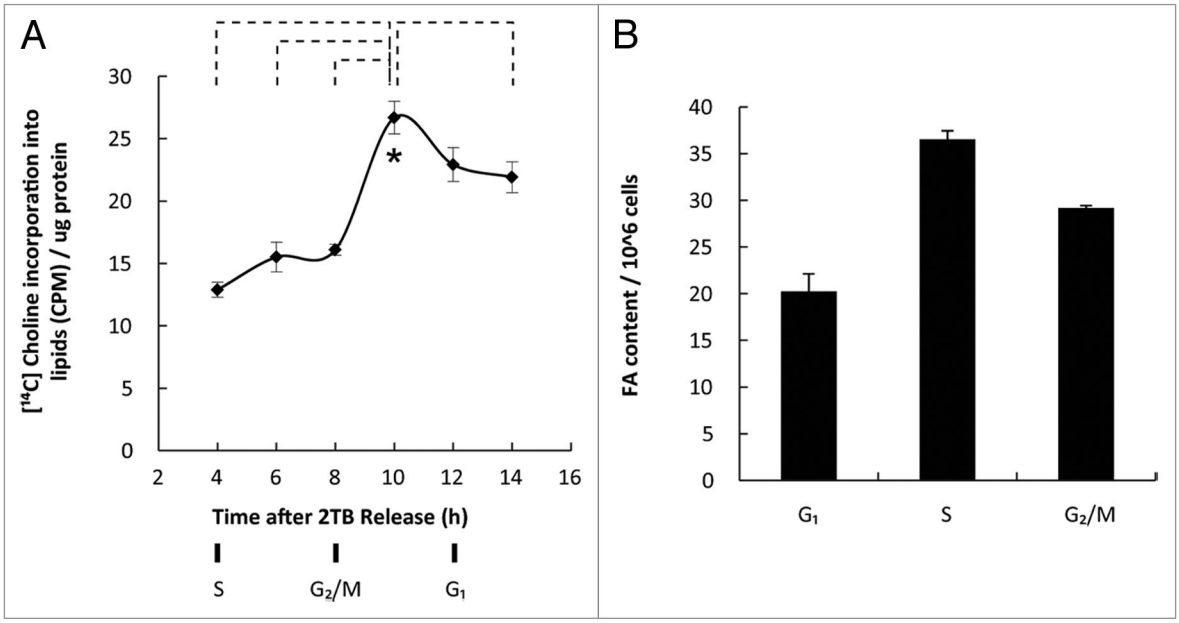

Figure 2. Membrane synthesis increases from G_2/M to G_1. The cells were synchronized by 2TB. (**A**) Cells were pulsed with [^{14}C]choline for 2 h prior their harvesting, and the radioactivity associated to the lipid fraction was determined by scintillation counting and normalized to total protein content. (**B**) The total fatty acid content at G_1 (12 h), S (4 h), and G_2/M (8 h) was determined by gas chromatography using C23:0 as internal standard and normalized to cell number. The values are plotted as mean ± SD of a representative experiment. *P < 0.05 ANOVA and Tukey.

protein content (**Fig. S6**) of any of the enzymes tested through the cell cycle. The rate-limiting enzyme of de novo FA synthesis, ACC, is inactivated by AMPK-directed phosphorylation on the S79 residue. To accurately estimate the phosphorylation status of AMPK and ACC from mitosis to G_1, we synchronized the cells at early mitosis by thymidine–nocodazole treatment. In thymidine–nocodazole-synchronized cells, AMPK and ACC were highly phosphorylated at time 0 (nocodazole block) (**Fig. 5A**). pAMPK decreased rapidly upon cell cycle release, as did its target, pACC (**Fig. 5A**), which occurred just prior to cytokinesis initiation (**Fig. 5B**, right panel) . Both increased again as the cells reached G_1 phase after 2 h (**Fig. 5B**, left panel). As expected, the synthesis of FA during this period mirrored the ACC phosphorylation status (**Fig. 5C**) Moreover, continuous activation of AMPK by the new small molecule MT 63–78[36] caused an increase in cells with G_2/M amount of DNA, which was not reverted by the addition of exogenous palmitate (**Fig. 5D**) Furthermore, the inhibition of fatty acid synthesis downstream of ACC (by C75) arrested the cells at some interval between metaphase and telophase, when cyclin B1 was still high (**Fig. 4C**) but pAMPK/pACC

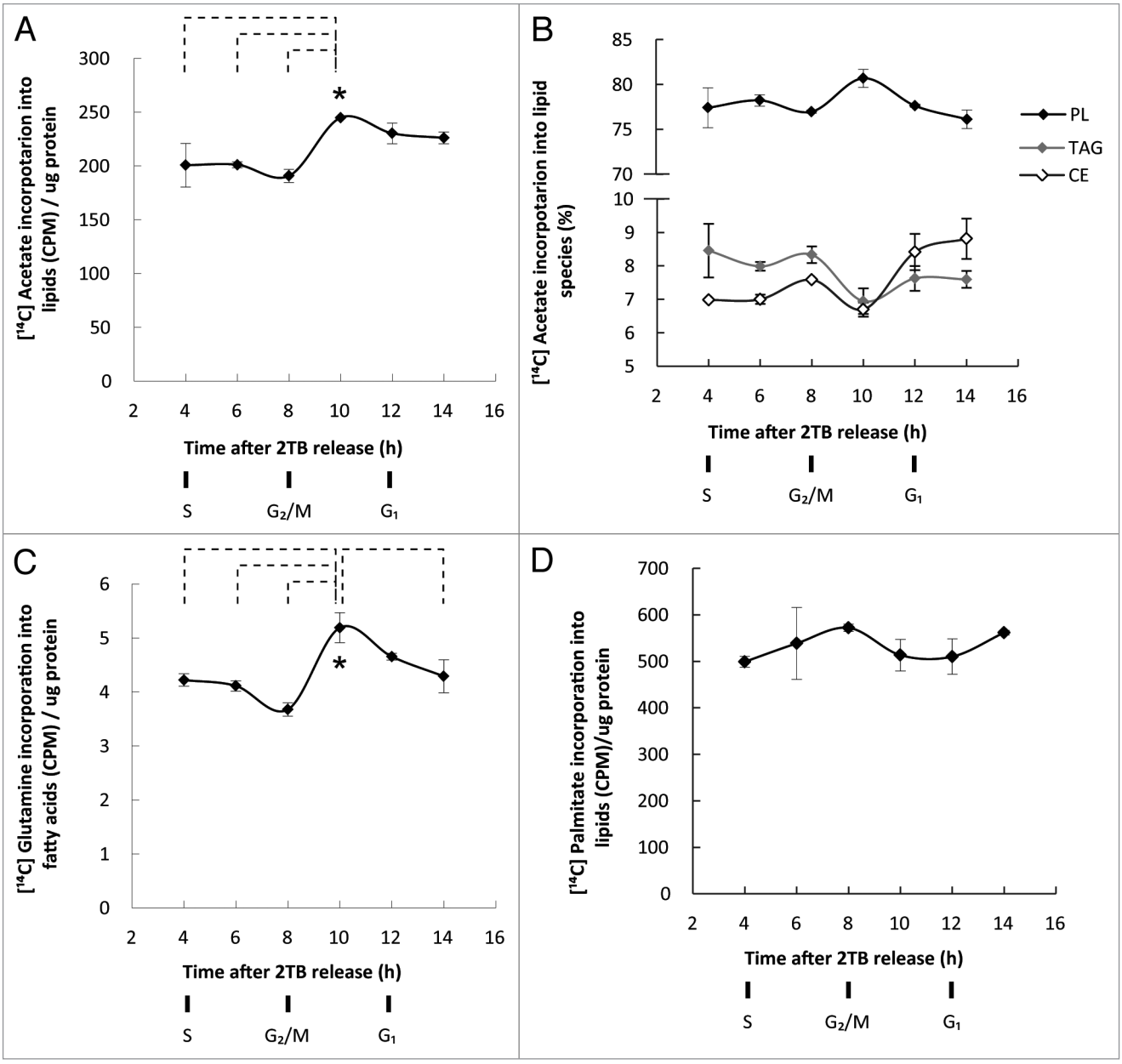

Figure 3. De novo fatty acid synthesis, but not the incorporation of exogenous fatty acids, increases as the cells divide. HeLa cells were synchronized by 2TB and released with fresh media as described under "Materials and Methods". The cells were pulsed with (**A**) [14C]acetate, (**C**) [14C]glutamine, or (**D**) [14C]palmitate for 2 h prior their harvesting. The radioactivity associated to the lipid fraction was determined by scintillation counting and normalized to total protein content. (**B**) The incorporation of [14C]acetate into different lipid species was estimated by thin layer chromatographic analysis of total lipids and scintillation counting. The values are plotted as mean ± SD of a representative experiment (except for [**B**], in which only one experiment was done). *$P < 0.05$ ANOVA and Tukey.

levels were low (**Fig. 5E**), suggesting that the final products of the pathway (de novo synthesized FA) were required to progress to G_1, independently of the pAMPK-ACC status. These results suggest that the increase in FA synthesis may be regulated by the induction of ACC activity driven by a decreased AMPK activation at the end of mitosis.

Discussion

Utilizing a synchronized population of cancer cells, we have shown that a decrease in LysoPL content from G_2/M to G_1 was accompanied by an increase in the de novo synthesis of FA, substrates for PL production, and phosphatidylcholine, the main PL in mammalian membranes, suggesting that a coordinated decrease in membrane turnover and increased PL synthesis occurred at the mitotic exit. Moreover, we showed that the inhibition of FA synthesis arrested the cells at G_2/M, probably at early M, indicating that membrane production started before G_1 and was necessary to complete cellular division. The incorporation of exogenous FA did not change during the cell cycle, nor did their depletion affect the cell cycle distribution, supporting the notion that endogenously synthesized FA are required to sustain cellular proliferation.

How these changes in lipid metabolism are coordinately regulated at the mitotic exit is yet to be determined. To this end, we showed that the activity of AMPK toward its metabolic target ACC is high at the beginning of mitosis and decreases at the end of it, in a manner consistent with the dynamics of the de novo FA synthesis. Continuous activation of AMPK by a small molecule led to an increase of cells with G_2/M amount of DNA, indicative of mitotic arrest. Previous studies have shown that AMPK associates with the mitotic apparatus[37] and regulates

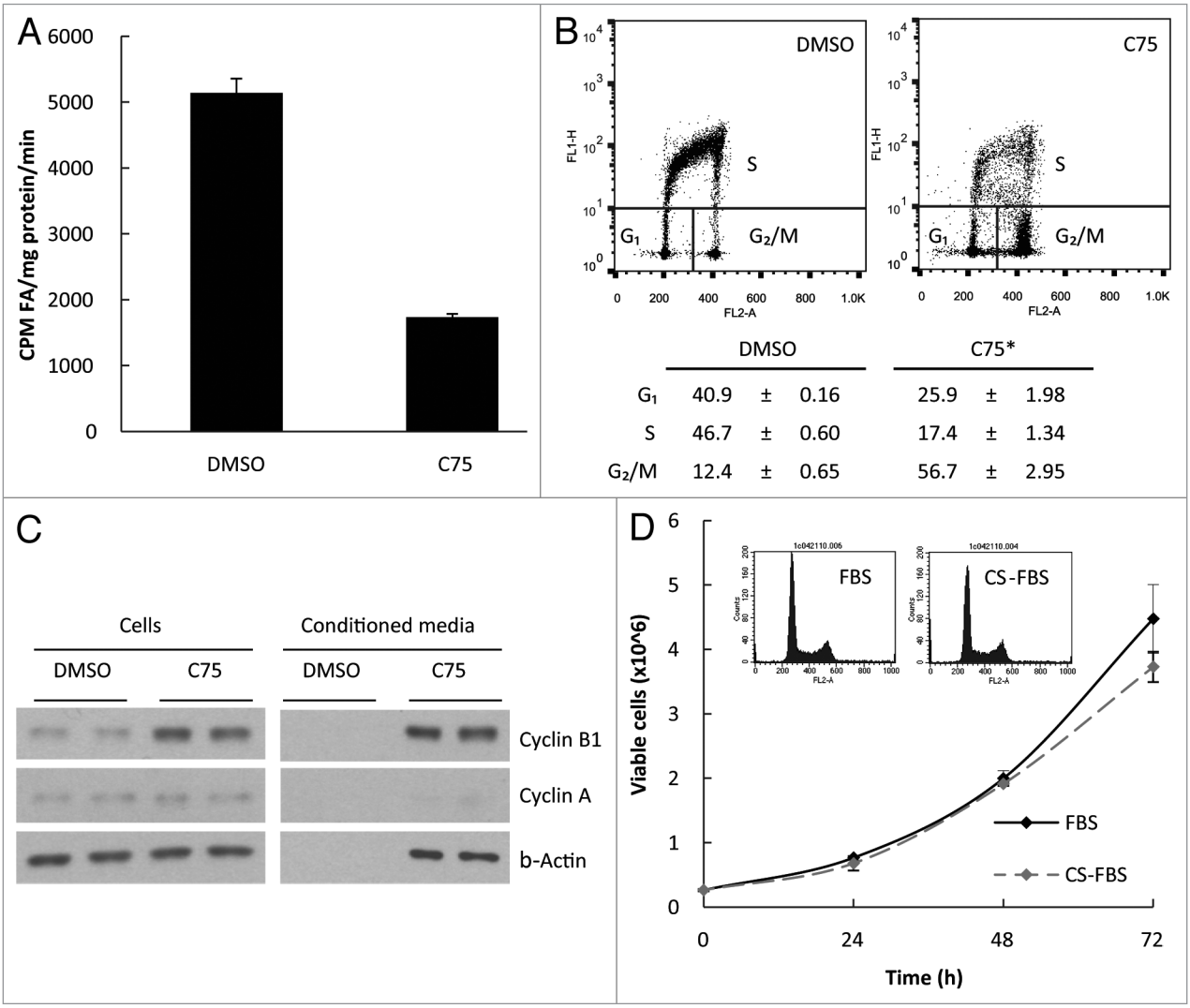

Figure 4. Impaired fatty acid synthesis, but not exogenous fatty acid depletion, arrests the cells at G_2/M. HeLa cells were incubated with 20 μg/ml of fatty acid synthase inhibitor (C75) or vehicle (DMSO) for 24 h. Cell extracts were assayed for FASN activity (**A**). Alternatively, the cells were pulsed with BrdU and the cell cycle distribution was assessed by FACS (**B**) and immunoblotting analysis of cyclins levels (**C**). To assess the importance of exogenous fatty acids for cell cycle progression, the cells were incubated with regular or charcoal-stripped FBS (CS-FBS) for 24 h and analyzed by FACS (**D**, inset). The sustained effect of exogenous lipid depletion on proliferation was estimated by counting of cells grown in CS-FBS for up to 72 h (**D**). *$P < 0.0001$ Chi-square and Fisher Exact Test (**B**).

several proteins related in mitosis and cytokinesis.[23] Therefore, it is likely that AMPK orchestrates the completion of mitosis by coordinately regulating chromosomal segregation, cytoskeleton rearrangement, and membrane synthesis.

Overall, our study shows that extensive changes in FA and PL metabolism occur during mitotic exit. Our data challenge and to some extent complement the current view in which lipid accumulation occurs only at S phase.[38] Our results are consistent with a biphasic model of PL/FA accumulation: one phase classically associated with cellular growth and another, from G_2/M to G_1, necessary to complete cellular division (**Fig. 6**). This model helps to explain the repeatedly observed phenomenon that the impairment of FA synthesis causes cell cycle arrest at G_2/M in yeast[39,40] and mammalian cells.[41-43] Moreover, the knockdown of fatty acid synthase as well as a choline deficient-diet alters the expression of genes important for G_2/M progression and cytokinesis in human cells.[44,45] LysoPL analogs, which alter both phosphatidylcholine synthesis and turnover,[46] also induce cell cycle arrest at G_2/M or at G_1 and G_2/M in different cancer and transformed cells.[47-49] Importantly, the arrest point depends on the time when the lipid perturbation starts (after or before the G_1/S boundary),[48] highlighting the 2 "lipogenic checkpoints" (**Fig. 6**).

The increasing interest in lipogenic enzymes as possible targets for cancer treatment and the development of inhibitors for this pathway[20,21,50,51] together with those for cell cycle-related kinases raises the possibility of combined therapy. In this context, the arrest at G_2/M caused by the reduction in PL/FA synthesis might be especially important for therapeutic intervention in p53-deficient cells, since their G_1 arrest checkpoint is impaired.[52,53] The knowledge of the metabolic requirements during the cell cycle and the effect of metabolic perturbations on cell cycle progression will be necessary for the design of therapeutic schedules and may be determinant of its outcome.[31]

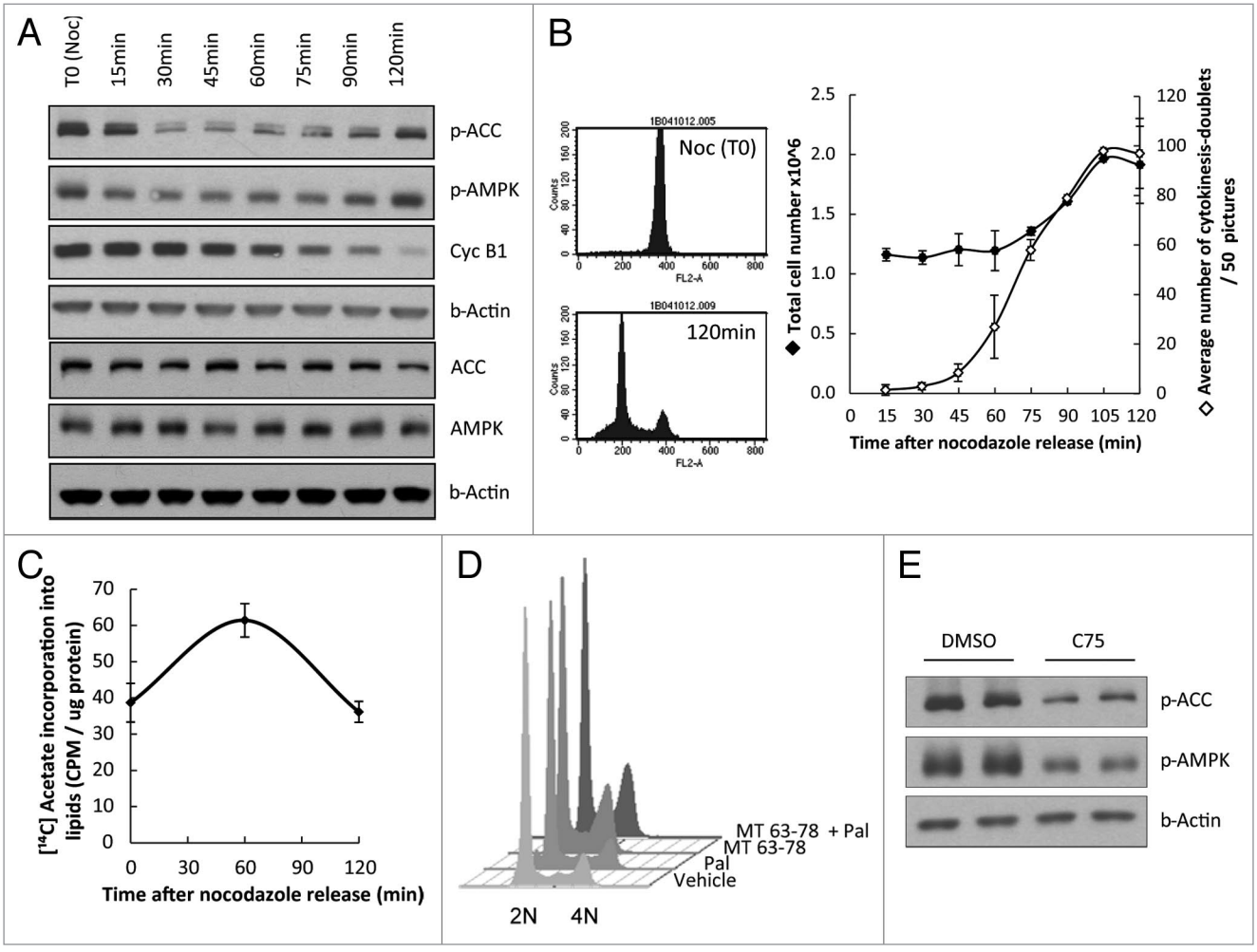

Figure 5. AMPK-mediated inhibitory phosphorylation of Acetyl-CoA Carboxylase decreases as the cells divide. HeLa cells, synchronized at early mitosis by thymidine-nocodazole block, were released and harvested every 15 min. The levels of pAMPK and pACC were assessed by western blot (**A**). The initiation and completion of cytokinesis was determined by counting hourglass-shaped cells and doublets, total cell number and by FACS analysis (**B**). The incorporation of [^{14}C] acetate into lipids was estimated with 30 min pulse in nocodazole-blocked (time cero) or released cells (**C**). HeLa cells were incubated with the AMPK activator MT 63–78 (25 μM) for 24 h in the presence or absence of 100 μM palmitic acid (with BSA in a 2:1 molar ratio), and cell cycle profile was assessed (**D**). Alternatively, cells were incubated with 20 μg/ml of fatty acid synthase inhibitor (C75) or vehicle (DMSO) for 24 h and pAMPK and pACC levels were assessed by western blot (**E**).

Materials and Methods

Cell culture and synchronization

Among several cellular models and synchronization protocols, we achieved highly synchronized populations only with HeLa cells (**Table S2**), thus we used this cell line for our synchronization experiments. HeLa cells were routinely grown in DMEM supplemented with 10% FBS, 100 units penicillin/ml, and 100 μg streptomycin /ml (P/S), 37 °C, 5% CO_2, and 100% humidity. One week prior to seeding for the experiments, the media changed to low glucose DMEM, which approximates normal blood glucose levels in vivo, supplemented with 10% FBS and P/S. Unless otherwise stated, 3.2×10^5 HeLa cells were seeded in 60-mm dishes and allowed to grow for 24 h. Cells were synchronized at the G_1/S boundary by double thymidine block (2TB) or at mitosis by thymidine–nocodazole block as previously described.[54] A brief description is provided in **Supplemental Methods**.

Cell cycle analysis

HeLa cells were incubated with 10 μM 5-Bromo-2'-deoxyuridine (BrdU) for 1–2 h before harvesting. Cells were processed for FACS analysis using FICT-conjugated anti-BrdU antibody (BD Biosciences) according to the manufacturers' directions in a FACScan flow cytometer (Becton Dickinson) and analyzed with ModFit or FlowJo software. For the estimation of cytokinesis initiation, thymidine–nocodazole-synchronized cells were harvested every 15 min, and the number of hourglass-shaped cells or doublets were counted from 50 images.

Metabolic profiling and data deconvolution

1.33×10^6 HeLa cells were seeded in quintuplicate 150-mm dishes, synchronized by 2TB, and harvested at the indicated time points. Cells were trypsinized and aliquots were used for protein determination. The remaining sample was kept at −80 °C until processed by Metabolon, as described Sreekumar et al.[55] The metabolite levels were normalized to the total protein content and deconvoluted as follows. For the analysis we used metabolites that had at least 3 measurements for each time point. To estimate average levels of each metabolite at each stage of the cell cycle we fitted a robust linear regression model of the form:

$$Y^m{}_i = \beta^S X_i^S + \beta^{G1} X_i^{G1} + \beta^{G2/M} X_i^{G2/M} + \tau_i + \varepsilon_i$$

where Y^m are observed levels of m-th metabolite, and X^S, X^{G1}, $X^{G2/M}$ are observed fractions of the cells in each phase of the cycle at the

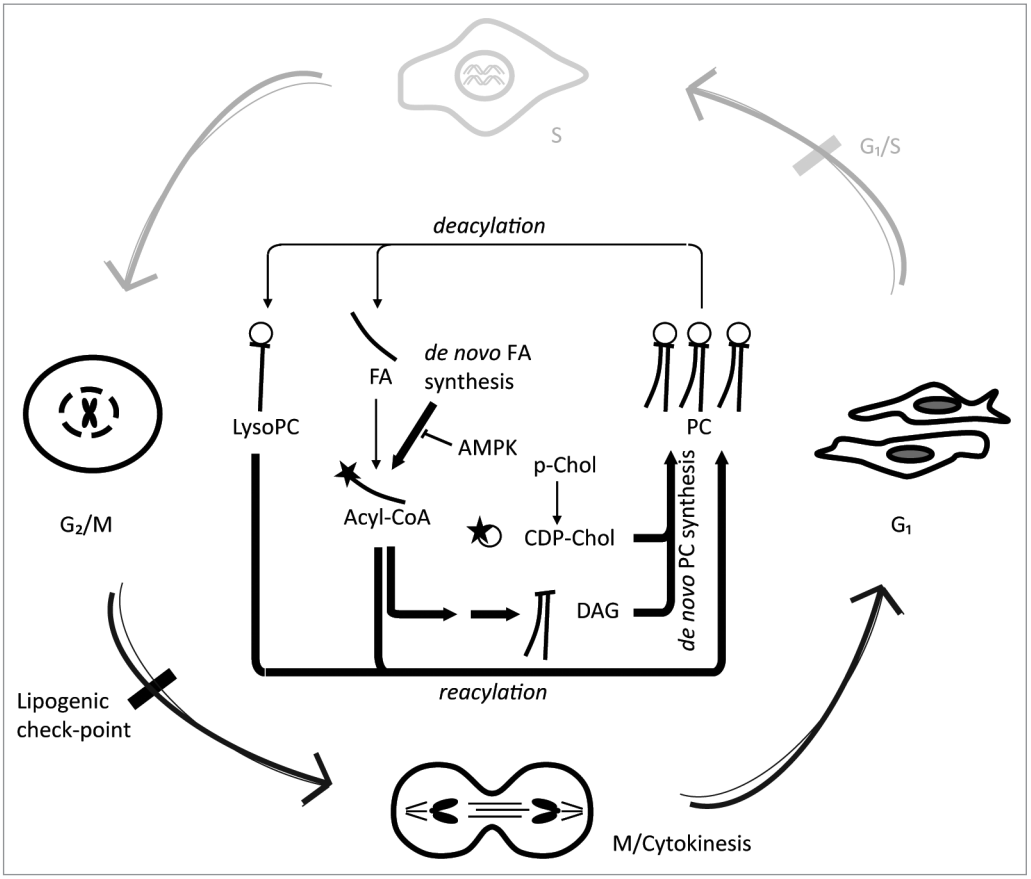

Figure 6. Model showing the coordinated changes in lipid metabolism that support membrane synthesis from G_2/M to G_1 phase of the cell cycle. De novo FA synthesis increases from G_2/M to G_1 to support de novo phosphatidylcholine synthesis. During this time, the reacylation rate of LysoPC surpasses PC deacylation, thus contributing to membrane accumulation (thick arrows). A reduction in AMPK-mediated inhibition of de novo FA synthesis (dashed line) may coordinately regulate membrane synthesis and mitosis progression. An impaired membrane synthesis arrests the cells at G_2/M, probably before ana/telophase, suggesting the presence of a "lipogenic checkpoint." For simplicity the lipid metabolism from G_1 to S and from S to G_2/M are not depicted (gray). FA, fatty acid; LysoPC, lysophosphatidylcholine; P-Chol, phosphocholine; CDP-Chol, CDP-choline; DAG, diacylglycerol; PC, phosphatidylcholine.

time of harvesting (FACS analysis). Time of cell harvesting was also included in the model (τ), as it provided a more accurate fit to the data. Estimated coefficients β^{S}, β^{G1}, and $\beta^{G2/M}$ represent deconvoluted average values for metabolite levels at S, G_1, and G_2/M phase, respectively. Metabolites were considered to be changing in a cell cycle-dependent manner if the coefficient of variation of the estimated average levels was above the 75th percentile, and if the maximum fold change between any pair of the stages of the cell cycle was above the median. Next, inferred average levels of these metabolites were standardized across the cell cycle stages and clustered using PAM (partitioning around medoids) algorithm. Six clusters provided the best clustering, as assessed by silhouette plots.

Metabolic labeling and lipid analysis

Cells were synchronized as described above by 2TB, released from the blockage in fresh media, and harvested after 4 h and every 2 h thereafter for up to 14 h. Two hours prior to harvesting, cells were labeled with 1–2 μCi/dish of either [1-^{14}C] acetic acid, [U-^{14}C] glutamine, [1-^{14}C] palmitic acid with 0.5% w/v bovine serum albumin, or [Methyl-^{14}C] choline (American Radiolabeled Chemicals) in growing media. Alternatively, the cells were synchronized by thymidine-nocodazole, released in fresh media (or fresh nocodazole-supplemented media, time 0), and labeled for 30 min with 3 μCi/dish [1-^{14}C] Acetic acid at the indicated time point. The lipids were extracted as described by Bligh and Dyer[56] and analyzed as described in reference 57. A brief description is provided in "Supplemental Methods". For total fatty acid quantification, the cellular lipids were transesterified with 10% boron trifluoride in methanol for 1 h at 100 °C under a nitrogen atmosphere. The derivative methyl esters were separated by gas–liquid chromatography at the Laboratory for Lipid Medicine and Technology (LLMT), Massachusetts General Hospital,Harvard Medical School, and quantified using 23:0 as internal standard.

FASN activity

Subconfluent cells were treated with C75 20 μg/ml (or DMSO vehicle) for 24 h. Cells were lysed in hypotonic buffer (1 mM DTT, 1 mM EDTA, 20 mM TRIS-HCl pH 7.5) and incubated at room temperature for 15 min. Twenty micrograms of proteins were preincubated at 37 °C for 2 min with NADPH solution (100 mM potassium phosphate pH 7, 100 mM KCl, 0.5 mM NADPH). The reaction was started by the addition of the substrate mixture (25 nmol Acetyl-CoA, 25 nmol Malonyl-CoA, 0.05 uCi [2–^{14}C] Malonyl-CoA, 164 uM final concentration of Acetyl- and Malonyl-CoA) and allowed to proceed for 10 min at 37 °C. The reaction was stopped with the addition of ice-cold 1 N HCl:MOH (6:4 v/v). Fatty acids were extracted with petroleum benzin, and the radioactivity was determined by scintillation counting.

Dependence on FA

Subconfluent cells were treated with C75 20 μg/ml (or DMSO vehicle) for 24 h. Two hours prior to harvesting, the cells were incubated with BrdU and analyzed by FACS as described above. Alternatively, cells and conditioned media were harvested for immunoblotting analysis or cell number and viability determination using a Vi-Cell counter (Beckman). For the analysis of the exogenous FA dependence, cells were grown in 10% regular or charcoal stripped FBS (CS-FBS) supplemented media. Cell number, viability, and cell cycle distribution were estimated as described above.

Incubation with AMPK activator

Subconfluent cells were treated with 25 μM AMPK activator MT 63-78 (Mercury Pharmaceuticals, Inc.) or DMSO vehicle with or without 100 μM palmitic acid (complexed with BSA in a 2:1 ratio) for 24 h. Cell cycle profile was assessed by FACS analysis with propidium iodide staining.

Immunoblotting

Cells were lysed in 1% NP-40 buffer with phosphatases and protease inhibitors. The lysates were cleared by centrifugation and 20 μg of protein, resolved on 4–12% Tris-glycine SDS-polyacrylamide gels, were transferred to Hybond nitrocellulose membrane. The following antibodies were used: anti-cyclin B1, anti-D1, anti-phospho-Cdc2 (Tyr15), anti-phospho-ACC (Ser79), anti-ACC, anti-AMPKα, anti-phospho AMPKα (Thr172) (Cell signaling), anti-FASN (BD Transduction laboratories), anti-Cyclin A (Santa Cruz Technology), anti-β-actin (Sigma).

Protein quantification

Total cellular protein content was quantified by the Bradford protein assay from Bio-Rad using bovine serum albumin as standard.

Statistical analysis

Statistically significant differences were assessed by one-way ANOVA and Tukey post-hoc test or Chi-square and Fisher Exact Test.

Disclosure of Potential Conflicts of Interest

No potential conflicts of interest were disclosed.

Acknowledgments

We are in debt to Dr Lesley Wassef for critical review of the manuscript and María Elina Scaglia for her help with the figures. This work was supported by the Prostate Cancer Foundation, the DF/HCC SPORE in Prostate Cancer (NIH/NCI P50 CA90381), NIH grant RO1CA131945, and philanthropic funds from Nuclea Biomarkers (Pittsfield, MA) to M.L.

Supplemental Materials

Supplemental materials may be found here:
www.landesbioscience.com/journals/cc/article/27767

References

1. Bergeron JJ, Warmsley AM, Pasternak CA. Phospholipid synthesis and degradation during the life-cycle of P815Y mast cells synchronized with excess of thymidine. Biochem J 1970; 119:489-92; PMID:5500308
2. Warmsley AM, Pasternak CA. The use of conventional and zonal centrifugation to study the life cycle of mammalian cells. Phospholipid and macromolecular synthesis in neoplastic mast cells. Biochem J 1970; 119:493-9; PMID:5500309
3. Graham JM, Sumner MC, Curtis DH, Pasternak CA. Sequence of events in plasma membrane assembly during the cell cycle. Nature 1973; 246:291-5; PMID:4271386; http://dx.doi.org/10.1038/246291a0
4. Jackowski S. Coordination of membrane phospholipid synthesis with the cell cycle. J Biol Chem 1994; 269:3858-67; PMID:8106431
5. Northwood IC, Tong AH, Crawford B, Drobnies AE, Cornell RB. Shuttling of CTP:Phosphocholine cytidylyltransferase between the nucleus and endoplasmic reticulum accompanies the wave of phosphatidylcholine synthesis during the G(0) --> G(1) transition. J Biol Chem 1999; 274:26240-8; PMID:10473578; http://dx.doi.org/10.1074/jbc.274.37.26240
6. Golfman LS, Bakovic M, Vance DE. Transcription of the CTP:phosphocholine cytidylyltransferase alpha gene is enhanced during the S phase of the cell cycle. J Biol Chem 2001; 276:43688-92; PMID:11557772; http://dx.doi.org/10.1074/jbc.M108170200
7. Manguikian AD, Barbour SE. Cell cycle dependence of group VIA calcium-independent phospholipase A2 activity. J Biol Chem 2004; 279:52881-92; PMID:15385540; http://dx.doi.org/10.1074/jbc.M410659200
8. Banchio C, Schang LM, Vance DE. Phosphorylation of Sp1 by cyclin-dependent kinase 2 modulates the role of Sp1 in CTP:phosphocholine cytidylyltransferase alpha regulation during the S phase of the cell cycle. J Biol Chem 2004; 279:40220-6; PMID:15247247; http://dx.doi.org/10.1074/jbc.M406468200
9. Tercé F, Brun H, Vance DE. Requirement of phosphatidylcholine for normal progression through the cell cycle in C3H/10T1/2 fibroblasts. J Lipid Res 1994; 35:2130-42; PMID:7897311
10. Cui Z, Houweling M, Chen MH, Record M, Chap H, Vance DE, Tercé F. A genetic defect in phosphatidylcholine biosynthesis triggers apoptosis in Chinese hamster ovary cells. J Biol Chem 1996; 271:14668-71; PMID:8663247; http://dx.doi.org/10.1074/jbc.271.25.14668
11. Bluemink JG, de Laat SW. New membrane formation during cytokinesis in normal and cytochalasin B-treated eggs of Xenopus laevis. I. Electron microscope observations. J Cell Biol 1973; 59:89-108; PMID:4356573; http://dx.doi.org/10.1083/jcb.59.1.89
12. Shuster CB, Burgess DR. Targeted new membrane addition in the cleavage furrow is a late, separate event in cytokinesis. Proc Natl Acad Sci U S A 2002; 99:3633-8; PMID:11891298; http://dx.doi.org/10.1073/pnas.052342699
13. Boucrot E, Kirchhausen T. Endosomal recycling controls plasma membrane area during mitosis. Proc Natl Acad Sci U S A 2007; 104:7939-44; PMID:17483462; http://dx.doi.org/10.1073/pnas.0702511104
14. Bosmann HB, Winston RA. Synthesis of glycoprotein, glycolipid, protein, and lipid in synchronized L5178Y cells. J Cell Biol 1970; 45:23-33; PMID:5458998; http://dx.doi.org/10.1083/jcb.45.1.23
15. Kobayashi T, Pagano RE. Lipid transport during mitosis. Alternative pathways for delivery of newly synthesized lipids to the cell surface. J Biol Chem 1989; 264:5966-73; PMID:2925644
16. Lin W, Arthur G. Phospholipids are synthesized in the G2/M phase of the cell cycle. Int J Biochem Cell Biol 2007; 39:597-605; PMID:17113814; http://dx.doi.org/10.1016/j.biocel.2006.10.011
17. Ellenberg J, Siggia ED, Moreira JE, Smith CL, Presley JF, Worman HJ, Lippincott-Schwartz J. Nuclear membrane dynamics and reassembly in living cells: targeting of an inner nuclear membrane protein in interphase and mitosis. J Cell Biol 1997; 138:1193-206; PMID:9298976; http://dx.doi.org/10.1083/jcb.138.6.1193
18. Anderson DJ, Hetzer MW. Nuclear envelope formation by chromatin-mediated reorganization of the endoplasmic reticulum. Nat Cell Biol 2007; 9:1160-6; PMID:17828249; http://dx.doi.org/10.1038/ncb1636
19. Kuhajda FP, Jenner K, Wood FD, Hennigar RA, Jacobs LB, Dick JD, Pasternack GR. Fatty acid synthesis: a potential selective target for antineoplastic therapy. Proc Natl Acad Sci U S A 1994; 91:6379-83; PMID:8022791; http://dx.doi.org/10.1073/pnas.91.14.6379
20. Kuhajda FP. Fatty acid synthase and cancer: new application of an old pathway. Cancer Res 2006; 66:5977-80; PMID:16778164; http://dx.doi.org/10.1158/0008-5472.CAN-05-4673
21. Flavin R, Peluso S, Nguyen PL, Loda M. Fatty acid synthase as a potential therapeutic target in cancer. Future Oncol 2010; 6:551-62; PMID:20373869; http://dx.doi.org/10.2217/fon.10.11
22. Zhang J, Yang Y, Wu J. Palmitate impairs cytokinesis associated with RhoA inhibition. Cell Res 2010; 20:492-4; PMID:20231861; http://dx.doi.org/10.1038/cr.2010.33
23. Banko MR, Allen JJ, Schaffer BE, Wilker EW, Tsou P, White JL, Villén J, Wang B, Kim SR, Sakamoto K, et al. Chemical genetic screen for AMPKα2 substrates uncovers a network of proteins involved in mitosis. Mol Cell 2011; 44:878-92; PMID:22137581; http://dx.doi.org/10.1016/j.molcel.2011.11.005
24. Bengoechea-Alonso MT, Punga T, Ericsson J. Hyperphosphorylation regulates the activity of SREBP1 during mitosis. Proc Natl Acad Sci U S A 2005; 102:11681-6; PMID:16081540; http://dx.doi.org/10.1073/pnas.0501494102
25. Bengoechea-Alonso MT, Ericsson J. Cdk1/cyclin B-mediated phosphorylation stabilizes SREBP1 during mitosis. Cell Cycle 2006; 5:1708-18; PMID:16880739; http://dx.doi.org/10.4161/cc.5.15.3131
26. Vander Heiden MG. Targeting cancer metabolism: a therapeutic window opens. Nat Rev Drug Discov 2011; 10:671-84; PMID:21878982; http://dx.doi.org/10.1038/nrd3504
27. Aguilar V, Fajas L. Cycling through metabolism. EMBO Mol Med 2010; 2:338-48; PMID:20721988; http://dx.doi.org/10.1002/emmm.201000089
28. Almeida A, Bolaños JP, Moncada S. E3 ubiquitin ligase APC/C-Cdh1 accounts for the Warburg effect by linking glycolysis to cell proliferation. Proc Natl Acad Sci U S A 2010; 107:738-41; PMID:20080744; http://dx.doi.org/10.1073/pnas.0913668107
29. Ray H, Suau F, Vincent A, Dalla Venezia N. Cell cycle regulation of the BRCA1/acetyl-CoA-carboxylase complex. Biochem Biophys Res Commun 2009; 378:615-9; PMID:19061860; http://dx.doi.org/10.1016/j.bbrc.2008.11.090
30. Wieprecht M, Wieder T, Paul C, Geilen CC, Orfanos CE. Evidence for phosphorylation of CTP:phosphocholine cytidylyltransferase by multiple proline-directed protein kinases. J Biol Chem 1996; 271:9955-61; PMID:8626633; http://dx.doi.org/10.1074/jbc.271.17.9955
31. Shah MA, Schwartz GK. Cell cycle-mediated drug resistance: an emerging concept in cancer therapy. Clin Cancer Res 2001; 7:2168-81; PMID:11489790
32. Bettuzzi S, Davalli P, Astancolle S, Pinna C, Roncaglia R, Boraldi F, Tiozzo R, Sharrard M, Corti A. Coordinate changes of polyamine metabolism regulatory proteins during the cell cycle of normal human dermal fibroblasts. FEBS Lett 1999; 446:18-22; PMID:10100606; http://dx.doi.org/10.1016/S0014-5793(99)00182-9
33. Brand K, Aichinger S, Forster S, Kupper S, Neumann B, Nürnberg W, Ohrisch G. Cell-cycle-related metabolic and enzymatic events in proliferating rat thymocytes. Eur J Biochem 1988; 172:695-702; PMID:3258238; http://dx.doi.org/10.1111/j.1432-1033.1988.tb13944.x
34. Geley S, Kramer E, Gieffers C, Gannon J, Peters JM, Hunt T. Anaphase-promoting complex/cyclosome-dependent proteolysis of human cyclin A starts at the beginning of mitosis and is not subject to the spindle assembly checkpoint. J Cell Biol 2001; 153:137-48; PMID:11285280; http://dx.doi.org/10.1083/jcb.153.1.137
35. Clute P, Pines J. Temporal and spatial control of cyclin B1 destruction in metaphase. Nat Cell Biol 1999; 1:82-7; PMID:10559878; http://dx.doi.org/10.1038/10049
36. Zadra G, Photopoulos C, Tyekucheva S, Heidari P, Weng QP, Fedele G, Liu H, Scaglia N, Priolo C, Sicinska E, et al. A novel direct activator of AMPK inhibits prostate cancer growth by blocking lipogenesis. EMBO Mol Med 2014; In press.
37. Vazquez-Martin A, Oliveras-Ferraros C, Menendez JA. The active form of the metabolic sensor: AMP-activated protein kinase (AMPK) directly binds the mitotic apparatus and travels from centrosomes to the spindle midzone during mitosis and cytokinesis. Cell Cycle 2009; 8:2385-98; PMID:19556893; http://dx.doi.org/10.4161/cc.8.15.9082
38. Jackowski S. Cell cycle regulation of membrane phospholipid metabolism. J Biol Chem 1996; 271:20219-22; PMID:8702749
39. Saitoh S, Takahashi K, Nabeshima K, Yamashita Y, Nakaseko Y, Hirata A, Yanagida M. Aberrant mitosis in fission yeast mutants defective in fatty acid synthetase and acetyl CoA carboxylase. J Cell Biol 1996; 134:949-61; PMID:8769419; http://dx.doi.org/10.1083/jcb.134.4.949
40. Al-Feel W, DeMar JC, Wakil SJ. A Saccharomyces cerevisiae mutant strain defective in acetyl-CoA carboxylase arrests at the G2/M phase of the cell cycle. Proc Natl Acad Sci U S A 2003; 100:3095-100; PMID:12626751; http://dx.doi.org/10.1073/pnas.0538069100
41. Li JN, Gorospe M, Chrest FJ, Kumaravel TS, Evans MK, Han WF, Pizer ES. Pharmacological inhibition of fatty acid synthase activity produces both cytostatic and cytotoxic effects modulated by p53. Cancer Res 2001; 61:1493-9; PMID:11245456
42. Gao Y, Lin LP, Zhu CH, Chen Y, Hou YT, Ding J. Growth arrest induced by C75, A fatty acid synthase inhibitor, was partially modulated by p38 MAPK but not by p53 in human hepatocellular carcinoma. Cancer Biol Ther 2006; 5:978-85; PMID:16855382; http://dx.doi.org/10.4161/cbt.5.8.2883
43. Horiguchi A, Asano T, Asano T, Ito K, Sumitomo M, Hayakawa M. Pharmacological inhibitor of fatty acid synthase suppresses growth and invasiveness of renal cancer cells. J Urol 2008; 180:729-36; PMID:18555493; http://dx.doi.org/10.1016/j.juro.2008.03.186
44. Knowles LM, Smith JW. Genome-wide changes accompanying knockdown of fatty acid synthase in breast cancer. BMC Genomics 2007; 8:168; PMID:17565694; http://dx.doi.org/10.1186/1471-2164-8-168
45. Niculescu MD, da Costa KA, Fischer LM, Zeisel SH. Lymphocyte gene expression in subjects fed a low-choline diet differs between those who develop organ dysfunction and those who do not. Am J Clin Nutr 2007; 86:230-9; PMID:17616785

46. Modolell M, Andreesen R, Pahlke W, Brugger U, Munder PG. Disturbance of phospholipid metabolism during the selective destruction of tumor cells induced by alkyl-lysophospholipids. Cancer Res 1979; 39:4681-6; PMID:498095
47. Engebraaten O, Bjerkvig R, Berens ME. Effect of alkyl-lysophospholipid on glioblastoma cell invasion into fetal rat brain tissue in vitro. Cancer Res 1991; 51:1713-9; PMID:1998962
48. Boggs KP, Rock CO, Jackowski S. Lysophosphatidylcholine attenuates the cytotoxic effects of the antineoplastic phospholipid 1-O-octadecyl-2-O-methyl-rac-glycero-3-phosphocholine. J Biol Chem 1995; 270:11612-8; PMID:7744800; http://dx.doi.org/10.1074/jbc.270.19.11612
49. Patel V, Lahusen T, Sy T, Sausville EA, Gutkind JS, Senderowicz AM. Perifosine, a novel alkylphospholipid, induces p21(WAF1) expression in squamous carcinoma cells through a p53-independent pathway, leading to loss in cyclin-dependent kinase activity and cell cycle arrest. Cancer Res 2002; 62:1401-9; PMID:11888912
50. Igal RA. Stearoyl-CoA desaturase-1: a novel key player in the mechanisms of cell proliferation, programmed cell death and transformation to cancer. Carcinogenesis 2010; 31:1509-15; PMID:20595235; http://dx.doi.org/10.1093/carcin/bgq131
51. Tong L, Harwood HJ Jr. Acetyl-coenzyme A carboxylases: versatile targets for drug discovery. J Cell Biochem 2006; 99:1476-88; PMID:16983687; http://dx.doi.org/10.1002/jcb.21077
52. De Witt Hamer PC, Mir SE, Noske D, Van Noorden CJ, Würdinger T. WEE1 kinase targeting combined with DNA-damaging cancer therapy catalyzes mitotic catastrophe. Clin Cancer Res 2011; 17:4200-7; PMID:21562035; http://dx.doi.org/10.1158/1078-0432.CCR-10-2537
53. Dixon H, Norbury CJ. Therapeutic exploitation of checkpoint defects in cancer cells lacking p53 function. Cell Cycle 2002; 1:362-8; PMID:12548006; http://dx.doi.org/10.4161/cc.1.6.257
54. Whitfield ML, Zheng LX, Baldwin A, Ohta T, Hurt MM, Marzluff WF. Stem-loop binding protein, the protein that binds the 3′ end of histone mRNA, is cell cycle regulated by both translational and posttranslational mechanisms. Mol Cell Biol 2000; 20:4188-98; PMID:10825184; http://dx.doi.org/10.1128/MCB.20.12.4188-4198.2000
55. Sreekumar A, Poisson LM, Rajendiran TM, Khan AP, Cao Q, Yu J, Laxman B, Mehra R, Lonigro RJ, Li Y, et al. Metabolomic profiles delineate potential role for sarcosine in prostate cancer progression. Nature 2009; 457:910-4; PMID:19212411; http://dx.doi.org/10.1038/nature07762
56. Bligh EG, Dyer WJ. A rapid method of total lipid extraction and purification. Can J Biochem Physiol 1959; 37:911-7; PMID:13671378; http://dx.doi.org/10.1139/o59-099
57. Scaglia N, Igal RA. Stearoyl-CoA desaturase is involved in the control of proliferation, anchorage-independent growth, and survival in human transformed cells. J Biol Chem 2005; 280:25339-49; PMID:15851470; http://dx.doi.org/10.1074/jbc.M501159200